

# Sex-specific regulation of *Lgr3* in *Drosophila* neurons

Geoffrey W. Meissner<sup>a</sup>, Shengzhan D. Luo<sup>a</sup>, Brian G. Dias<sup>a</sup>, Michael J. Texada<sup>a</sup>, and Bruce S. Baker<sup>a,1</sup>

<sup>a</sup>Janelia Research Campus, Howard Hughes Medical Institute, 19700 Helix Drive, Ashburn, VA 20147

Contributed by Bruce S. Baker, January 12, 2016 (sent for review September 29, 2015; reviewed by Artyom Kopp and Brian Oliver)

The development of sexually dimorphic morphology and the potential for sexually dimorphic behavior in *Drosophila* are regulated by the Fruitless (Fru) and Doublesex (Dsx) transcription factors. Several direct targets of Dsx have been identified, but direct Fru targets have not been definitively identified. We show that *Drosophila* leucine-rich repeat G protein-coupled receptor 3 (*Lgr3*) is regulated by Fru and Dsx in separate populations of neurons. *Lgr3* is a member of the relaxin-receptor family and a receptor for Dilp8, necessary for control of organ growth. *Lgr3* expression in the anterior central brain of males is inhibited by the B isoform of Fru, whose DNA binding domain interacts with a short region of an *Lgr3* intron. Fru A and C isoform mutants had no observed effect on *Lgr3* expression. The female form of Dsx (Dsx<sup>F</sup>) separately up- and down-regulates *Lgr3* expression in distinct neurons in the abdominal ganglion through female- and male-specific *Lgr3* enhancers. Excitation of neural activity in the Dsx<sup>F</sup>-up-regulated abdominal ganglion neurons inhibits female receptivity, indicating the importance of these neurons for sexual behavior. Coordinated regulation of *Lgr3* by Fru and Dsx marks a point of convergence of the two branches of the sex-determination hierarchy.

*Lgr3* | *fruitless* | *doublesex* | *Drosophila* | enhancer

Most animal species are comprised of female and male individuals, in which sex differences in form and behavior are specified by their genetic makeup. The developmental processes by which genes build sex-specific differences into the nervous system, and hence encode the potential for sex-specific behavior, have long been of interest (1).

In *Drosophila melanogaster* the assessment of the number of X chromosomes leads to sex-differential splicing of transcripts from genes making up the sex-determination hierarchy, in particular the terminal genes of that hierarchy, *fruitless* (*fru*) and *doublesex* [*dsx* (2), reviewed in ref. 3]. *fru* and *dsx* encode sex-specific Zn-finger transcription factors that alter, either directly or indirectly, the expression of downstream genes to produce the sexually dimorphic elements of flies. The male-specific forms of Fru (Fru<sup>M</sup>) act in a subset of the neurons within the male's nervous system to establish the potential for social interactions such as courtship behavior and aggression (reviewed in ref. 3). In contrast, Dsx acts in subsets of both neural and nonneural tissues of males and females to regulate behavioral and nonbehavioral aspects of sexual development (reviewed in ref. 3).

Although the mechanisms regulating the production of the sex-specific isoforms of the Fru and Dsx proteins are well-established (4), how these proteins in turn function is only beginning to be elucidated. Several direct Dsx targets and a well-conserved 13-bp Dsx binding site have been identified (5–13). Many Dsx target genes encode well-known transcription factors and cell-cell signaling molecules that function sex-nonspecifically in most tissues in which they are expressed. However, in other tissues, Dsx directs the sex-specific expression of these genes to generate sex-specific aspects of development.

Fru<sup>M</sup>'s regulatory function has thus far proven to be less tractable than that of Dsx. Fru<sup>M</sup> appears to function in a complex with the transcription cofactor Bonus and either histone deacetylase 1 or heterochromatin protein 1a (14). Recent genome-wide screens of RNA expression levels or Fru<sup>M</sup> binding activity have identified potential Fru<sup>M</sup> targets, but have lacked independent confirmation

of such regulation (15–17). Thus, our understanding of how Fru<sup>M</sup> specifies the potential for sex-specific behavior remains limited.

Along with the study of the genetic targets of Dsx and Fru<sup>M</sup>, studying the control of neuronal function by genomic enhancer elements has identified behavioral roles for Dsx- and Fru<sup>M</sup>-expressing neurons (3, 18–20). In a screen for additional genomic enhancer elements that drive sexually dimorphic nervous system expression, we identified an enhancer derived from the *Lgr3* gene. *Lgr3* is a member of the leucine-rich repeat G-protein-coupled receptor (Lgr) family, including *Lgr2*, encoded by the *ricketts* gene and necessary for tanning of the adult cuticle in response to the hormone bursicon (22). *Lgr*-related genes are also present in humans and include those encoding relaxin-family peptide receptors RXFP1 and RXFP2, which among other functions are necessary for normal reproduction in both sexes (reviewed in ref. 23).

We investigated the sex-specific regulation of *Lgr3* expression and its functional importance in female sexual behavior. We identified roles for both Fru<sup>M</sup> and Dsx in regulating *Lgr3* expression in separate sets of neurons. One isoform of Fru inhibits *Lgr3* expression in the male brain, whereas Dsx activates *Lgr3* expression in some neurons in the female abdominal ganglion and represses it in others. To better understand the basis of this complex regulation of *Lgr3* expression, potential enhancer fragments from the *Lgr3* locus were used to narrow down the sites of Fru and Dsx activity. We found that Fru<sup>M</sup> interacts with a specific portion of an *Lgr3* intron, suggesting its regulation may be direct. Finally, activation of a subset of *Lgr3*-expressing abdominal ganglion neurons reduced female receptivity to courtship, indicating the functional importance of sex-specific *Lgr3* expression.

## Results

We examined the expression of the *Lgr3* gene using a bacterial artificial chromosome (BAC) reporter, *Lgr3-GAL4::VP16*, encompassing the *Lgr3* locus, with the GAL4 DNA-binding domain and VP16 activation domain inserted in place of the first coding exon of *Lgr3* (Fig. 1A). *Lgr3-GAL4* drives expression of a *UAS-GFP*

## Significance

For individuals to develop sexually dimorphic body parts and behavior, their cells must know their sex. In the fruit fly *Drosophila melanogaster*, this process is carried out by a series of genes ending with *fruitless* (*fru*) and *doublesex* (*dsx*). We found that both Fru and Dsx regulate the expression of the leucine-rich repeat G protein-coupled receptor 3 (*Lgr3*) gene in separate sets of neurons, including neurons important for female sexual behavior. Thus, *Lgr3* is important for sexual development and is a point of convergence after the *fru/dsx* split.

Author contributions: G.W.M. and B.S.B. designed research; G.W.M. and S.D.L. performed research; B.G.D. and M.J.T. contributed new reagents/analytic tools; G.W.M. and S.D.L. analyzed data; and G.W.M. and B.S.B. wrote the paper.

Reviewers: A.K., University of California, Davis; and B.O., National Institutes of Health.

The authors declare no conflict of interest.

Freely available online through the PNAS open access option.

<sup>1</sup>To whom correspondence should be addressed. Email: bakerb@janelia.hhmi.org.

This article contains supporting information online at [www.pnas.org/lookup/suppl/doi:10.1073/pnas.1600241113/-DCSupplemental](http://www.pnas.org/lookup/suppl/doi:10.1073/pnas.1600241113/-DCSupplemental).

reporter in a sexually dimorphic pattern in the brain median bundle and in the abdominal ganglion (Fig. 1B). In the median bundle of both pupae and adults, *Lgr3-GAL4* is expressed in significantly more neurons in females than in males (Fig. 1G and Fig. S14).

To verify that the expression of the *Lgr3-GAL4* reporter accurately reflects expression of the *Lgr3* gene, we compared *Lgr3-GAL4*'s expression pattern to the pattern of in situ hybridization of *Lgr3* probes to transcripts in sections of males and females (Fig. 1C and Fig. S1B and C). *Lgr3* antisense probe signal colocalized with *Lgr3-GAL4* expression in both males and females, whereas the sense probe control lacked any observable coexpression (Fig. 1C). Expression of both GFP and the in situ probe appeared greater in females than males. Additional antisense probes targeting other regions of *Lgr3* showed a similar pattern (Fig. S1D). Although otherwise coexpressed, hybridization signal in the abdominal ganglion was present in a few cells beyond the *Lgr3-GAL4* pattern in both sexes.

**Fru<sup>M</sup> Inhibits Expression of *Lgr3* in the Male Median Bundle.** To understand the basis of sexually dimorphic *Lgr3* expression in the median bundle, we examined the dependence of *Lgr3-GAL4*

expression on Fru<sup>M</sup> and Dsx. Dsx expression has not been detected in the median bundle (24, 25), and *dsx* loss-of-function mutants had no effect on *Lgr3-GAL4* expression in the median bundle (Fig. S2). In contrast, Fru<sup>M</sup> is expressed in the median bundle (26), and we observed coexpression of a *LexA* reporter for fru<sup>M</sup> (*fru<sup>LexA</sup>*) (27) and *Lgr3-GAL4* when examined with fluorescent nuclear reporters in the median bundle (Fig. 1D). Similar coexpression was seen when *LexAop2-FlpL* and *UAS > stop > myrGFP* were used to perform Flippase-mediated genetic intersection, in which *fru-LexA* and *Lgr3-GAL4* are both needed to cause Flp to remove the stop codon in *UAS > stop > myrGFP* and the production of GFP (Fig. 1E). In a fru<sup>M</sup> loss-of-function mutant (*fru<sup>4-40</sup>/fru<sup>LexA</sup>*), *Lgr3-GAL4*, *UAS-GFP* expression in males was restored to nearly female levels, indicating that wild-type Fru<sup>M</sup> likely inhibits *Lgr3-GAL4* expression in males (Fig. 1F and G).

Differences in the numbers of cells expressing *Lgr3-GAL4* could be a result of *Lgr3-GAL4* expression being altered in existing cells, or to the death of some of those cells. Prior studies of Fru<sup>M</sup> expression reported cell number dimorphism in other subsets of Fru<sup>M</sup> neurons, but not in the median bundle (28, 29).

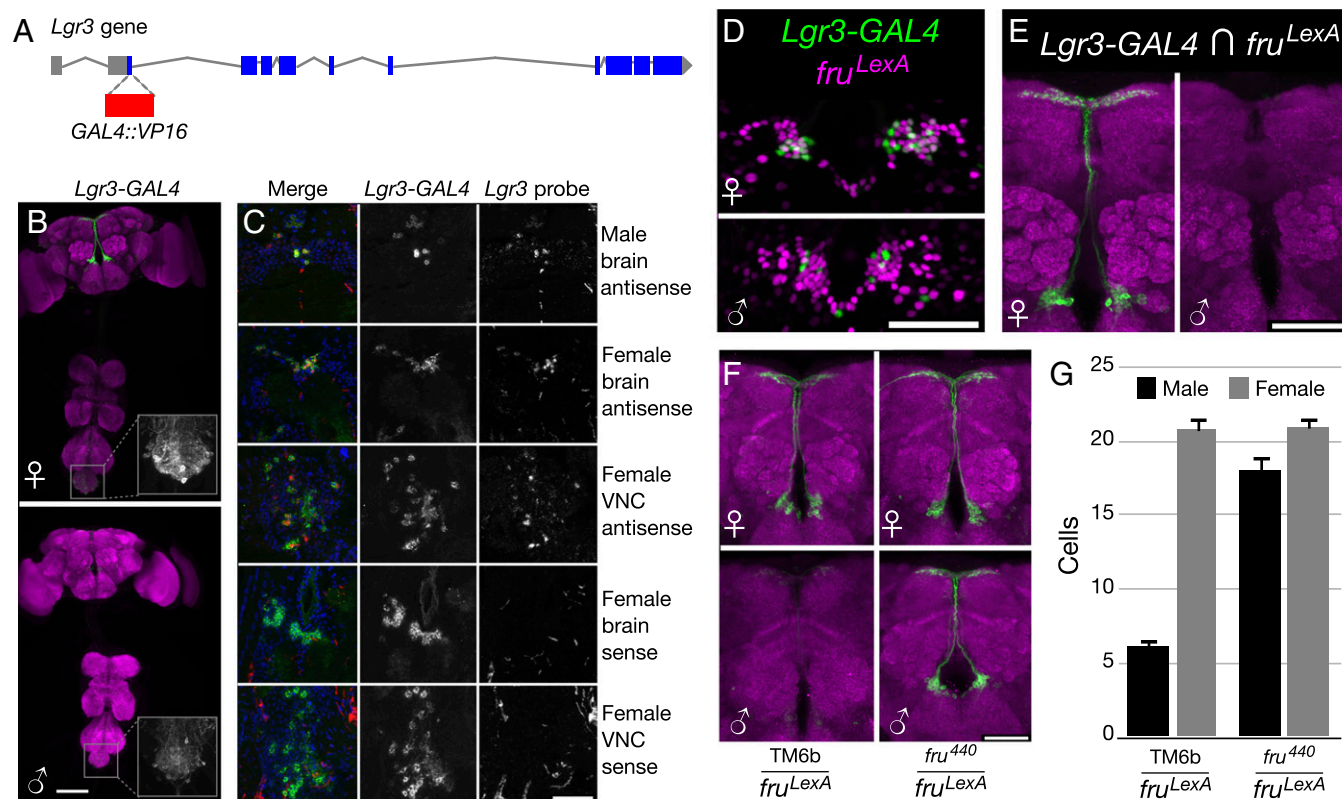


**Fig. 1.** Sexually dimorphic expression of *Lgr3*. (A) To create *Lgr3-GAL4::VP16*, *GAL4::VP16* was inserted into a BAC containing the *Lgr3* locus, along with ~1-kb upstream and 6.6-kb downstream sequence, the latter including several neighboring genes. Sequence encoding the GAL4 DNA-binding domain and VP16 activation domain replaced the first coding exon of *Lgr3*. (B) *Lgr3-GAL4* (*attP40*), *UAS-myrGFP* (*attP2*) shows higher expression in the female median bundle compared with the male median bundle. The brain and VNC were imaged in separate 20× tiles and composited. (Inset) *Lgr3-GAL4* expression in the abdominal ganglion at a higher gain and approximately 2.4× higher magnification. (Scale bar, 100 μm.) (C) DIG-labeled in situ hybridization of *Lgr3* antisense probe (in red) shows correspondence with *Lgr3-GAL4* (*attP40*), *UAS-myrGFP* (*su(Hw)attP5*) (in green) in horizontal sections through the male and female brain and abdominal ganglion. The sense probe did not show appreciable overlap with GFP. The membrane-bound GFP generally surrounds the mRNA signal in neurons with both labels. DAPI nuclear label (in blue) is included for reference. (Scale bar, 50 μm.) (D) *Lgr3-GAL4*, *UAS-Stinger-GFP* (green) overlaps with *fru<sup>LexA</sup>*, *LexAop > tdTomato* (magenta) in females, but less so in males. Overlap is in white. (Scale bar, 50 μm.) (E) Intersection of *Lgr3-GAL4* (*attP40*) with *fru<sup>LexA</sup>* using *LexAop2-FlpL* (*attP40*) and *UAS > stop > myrGFP* (*su(Hw)attP1*) leads to GFP expression primarily in females (8.6 ± 0.9 cells in females vs. 0.6 ± 0.2 in males,  $P < 0.001$  by Student's *t* test,  $n = 12-14$  hemispheres). GFP expression occurs only in cells expressing both *Lgr3* and *fru<sup>M</sup>*. (Scale bar, 50 μm.) (F) *Lgr3-GAL4* (*attP40*), *UAS-myrGFP* (*su(Hw)attP5*) shows dependence on Fru<sup>M</sup>. Elimination of Fru<sup>M</sup> function using *fru<sup>4-40</sup>/fru<sup>LexA</sup>* brings male expression close to female levels. (Scale bar, 50 μm.) (G) Cell counts for *F*. Expression in control females was significantly broader than in control males (20.6 ± 0.7 cells vs. 6.1 ± 0.7,  $P < 0.001$  by ANOVA and Tukey post hoc test,  $n = 8-10$  brain hemispheres). *fru<sup>4-40</sup>/fru<sup>LexA</sup>* male expression (17.9 ± 0.8) was significantly increased from control males ( $P < 0.001$ ), but still lower than in the female (20.9 ± 0.7), by a small amount ( $P < 0.01$ ). Error bars indicate SEM.

Cachero et al. (28) in particular counted the cells produced by neuroblast clones in both sexes and did not detect a difference. We verified that the number of Fru<sup>M</sup>-expressing median bundle neurons did not significantly differ between females and males ( $66.6 \pm 2.3$  cells vs.  $68.1 \pm 1.8$ ,  $P = 0.6$  by Student's  $t$  test,  $n = 22$ – $26$  hemispheres). Thus, differences in *Lgr3*-*GAL4* median bundle expression do not appear to result from cell death.

**Fru<sup>M</sup> Acts Through a Small Region of an *Lgr3* Intron.** To determine the region of the *Lgr3* locus through which Fru<sup>M</sup> regulates *Lgr3* median bundle expression, we asked whether various fragments of the *Lgr3* gene contained enhancer elements sufficient to confer Fru<sup>M</sup>-dependent enhancer-*GAL4* expression (Fig. 2A) (30). Of the five *Lgr3* fragments tested in this manner, only *R19B09*-*GAL4*, a fragment from the largest *Lgr3* intron, conferred sexually dimorphic median bundle expression similar to that exhibited by *Lgr3*-*GAL4* (Fig. S3). *R19B09* thus likely contains the enhancer sequences necessary for the median bundle expression observed with *Lgr3*. To further localize these enhancer sequences, we subdivided the 3,683-bp *R19B09*-*GAL4* reporter into smaller fragments, each of which was assayed for sexually dimorphic *GAL4* expression (Fig. 2B

and Fig. S3). Two rounds of such subdivisions yielded a 484-bp reporter termed *R19B09.3A*-*GAL4* that maintained dimorphic median bundle expression (Fig. 2B–D). As with *Lgr3*-*GAL4*, the expression of *R19B09.3A*-*GAL4* both colocalizes with *fru*-*LexA* in females and is inhibited by Fru<sup>M</sup> in males (Fig. 2E–H).

The *fru* gene encodes multiple transcripts through the use of alternative promoters in combination with sex-specific and sex-nonspecific alternative pre-mRNA splicing. The *fru* mRNAs thus generated are translated into proteins with different C-terminal Zn-finger DNA-binding domains. Of these, isoforms A, B, and C have detectable nervous system expression and are candidates for regulators of *Lgr3* expression in the male nervous system (31). We examined the expression of *R19B09.3A* in flies individually mutant for the A, B, or C isoforms (13, 28), and found that *R19B09.3A* expression was only affected by the absence of Fru<sup>B</sup> (Fig. 3A and B). Fru<sup>A</sup> and Fru<sup>C</sup> mutants had no effect on *R19B09.3A* expression, whereas in Fru<sup>B</sup> mutant males *R19B09.3A* expression is increased to female levels, suggesting that Fru<sup>B</sup> negatively affects *R19B09.3A*-dependent expression. Using pan-neuronally expressed microRNAs targeting transcripts of the A–C *fru* isoforms, we similarly observed that knockdown only of Fru<sup>B</sup> brought male expression to female

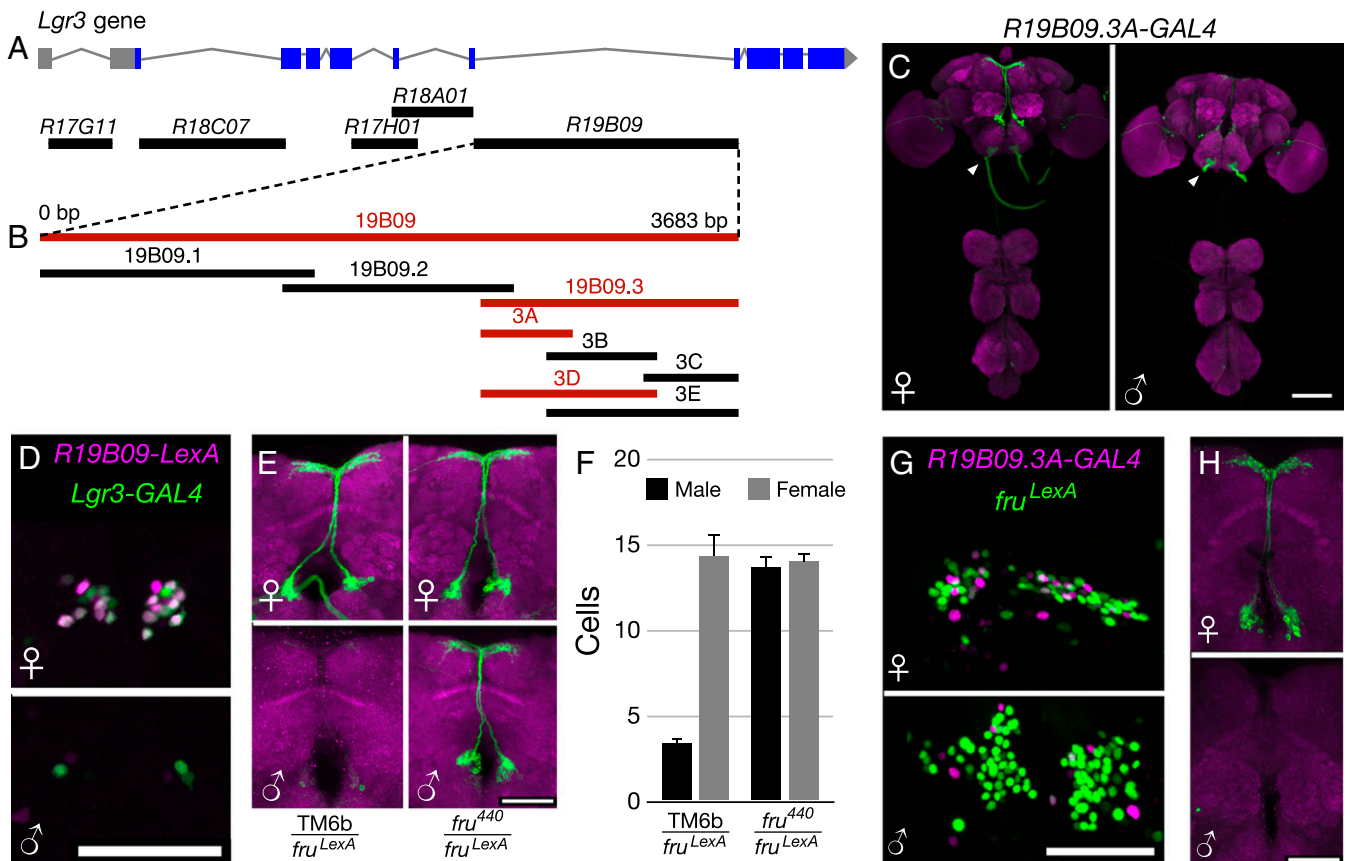


**Fig. 2. *R19B09.3A*-*GAL4* recapitulates dimorphic *Lgr3* median bundle expression.** (A) Rubin *GAL4* enhancer fragment lines contain sequences from the indicated regions of the *Lgr3* locus. (B) *R19B09*-*GAL4* was subdivided in two rounds to identify a smaller region driving dimorphic median bundle expression. Fragments in red showed dimorphic median bundle expression, whereas those in black had other patterns of expression (Fig. S3). (C) Expression of *R19B09.3A*-*GAL4*, *UAS-myrfGFP* (*attP40*) is sexually dimorphic in the female and male median bundle. *UAS-GFP* in (*attP40*) has basal expression in the labial nerve (arrowheads) (44). The brain and VNC were imaged in separate 20 $\times$  tiles and composited. (Scale bar, 100  $\mu$ m.) (D) *R19B09-LexA*, *LexAop2-IVS-nlstdTomato* (*VK22*) colocalizes with *Lgr3*-*GAL4*, *UAS-Stinger-GFP* in females, but both have low male expression. (Scale bar, 50  $\mu$ m.) (E) *R19B09.3A*-*GAL4* (*attP2*), *UAS-myrfGFP* (*attP40*) shows dependence on Fru<sup>M</sup>. Elimination of Fru<sup>M</sup> function using *fru*<sup>440</sup>/*fru*<sup>LexA</sup> brings male expression to female levels. (Scale bar, 50  $\mu$ m.) (F) Cell counts for E. Expression in control females was significantly broader than in males ( $14.2 \pm 0.8$  cells vs.  $3.4 \pm 0.5$ ,  $P < 0.001$  by ANOVA and Tukey post hoc test,  $n = 4$ – $10$  brain hemispheres). *fru*<sup>440</sup>/*fru*<sup>LexA</sup> male expression was indistinguishable from females ( $13.6 \pm 0.5$  vs.  $13.9 \pm 0.5$ ,  $P > 0.5$ ). Error bars indicate SEM. (G) *R19B09.3A*-*GAL4*, *UAS-RedStinger* colocalizes with *fru*<sup>LexA</sup>, *LexAop2-Stinger-GFP* in females but not males. (Scale bar, 50  $\mu$ m.) (H) Intersection of *R19B09.3A*-*GAL4* (*attP2*) with *fru*<sup>LexA</sup> using *LexAop2-F1pL* (*attP40*) and *UAS > stop > myrfGFP* (*su(Hw)attP1*) shows expression in females but not in males. (Scale bar, 50  $\mu$ m.)

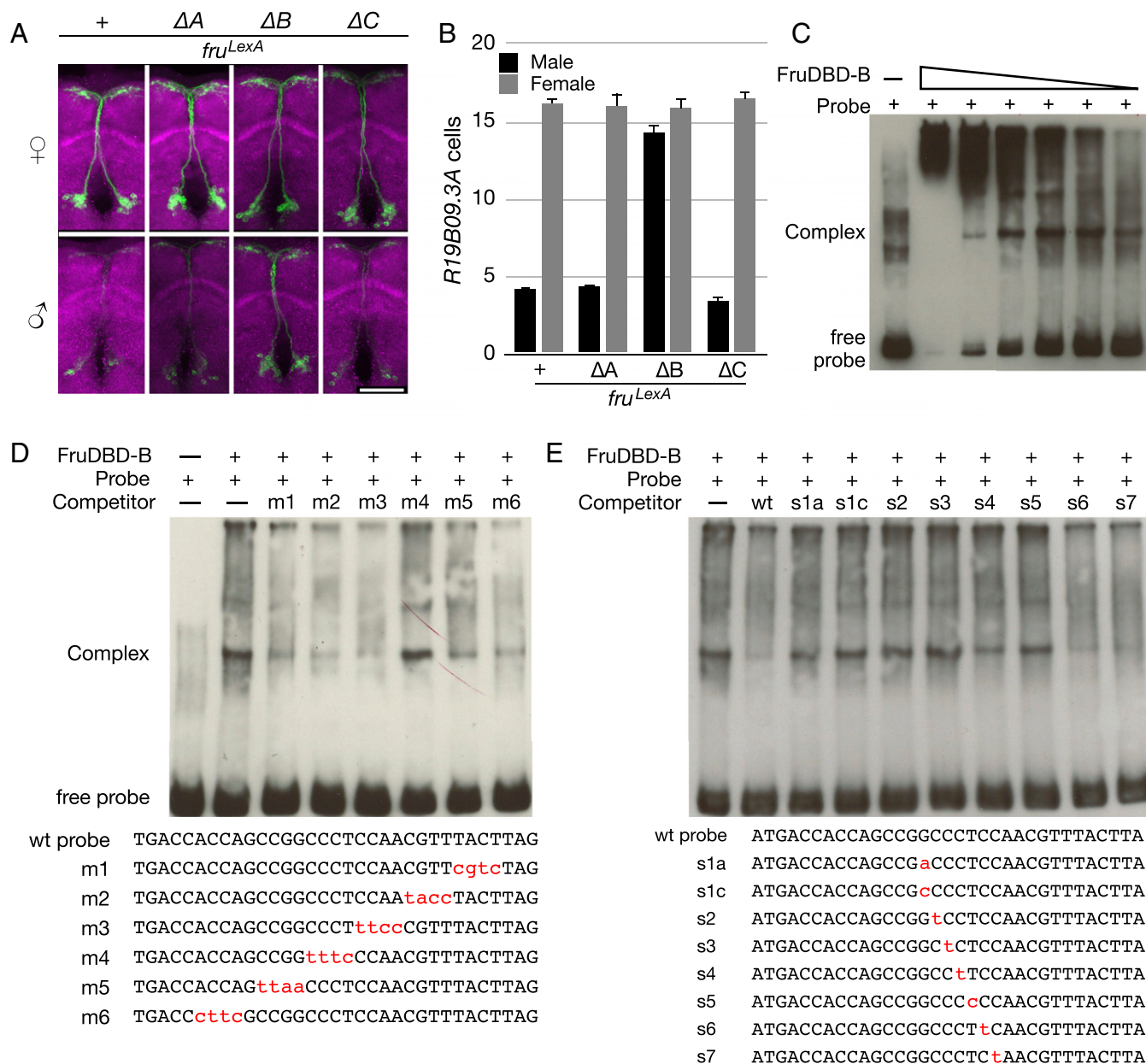


**Fig. 3.** Fru<sup>B</sup> regulates *R19B09.3A-GAL4* expression. (A) Expression of *R19B09.3A-GAL4*, *UAS-myrGFP (attP40)* in females and males carrying heteroallelic combinations of *fru<sup>LexA</sup>* with either a wild-type, *fru<sup>ΔA</sup>*, *fru<sup>ΔB</sup>*, or *fru<sup>ΔC</sup>* *fru* isoform mutant as indicated. (Scale bar, 50  $\mu$ m.) (B) Cell counts for A. Expression in males was significantly lower than in females for flies carrying heteroallelic combinations of *fru<sup>LexA</sup>* with either wild-type, *fru<sup>ΔA</sup>*, or *fru<sup>ΔC</sup>* ( $P < 0.001$  by Mann-Whitney  $u$  test with Bonferroni correction on each male/female pair,  $n = 18$ –30 hemispheres). However, in *fru<sup>LexA</sup>/fru<sup>ΔB</sup>* individuals the expression of *R19B09.3A-GAL4*, *UAS-myrGFP (attP40)* did not differ between males and females ( $P > 0.1$ ). Error bars indicate SEM. (C) EMSA showing binding of purified Fru-DBD-B protein to probe #3 from *R19B09.3A* (Fig. S5 C and D). A decreasing gradient in the amount of protein was used to show the binding kinetics. The bands for free probe and protein-DNA complex are indicated. (D) Tiled substitutions in a shorter probe derived from probe #3 were used as competitors in the EMSA to identify the specific position of Fru-DBD-B binding. The sequence of the labeled probe and the mutant sequences used as competitors are listed below the gel with the substituted nucleotides indicated in red lowercase. (E) Single base substitutions in the probe were used as competitors in the EMSA to examine the contribution of each position to the Fru-DBD-B binding site.

levels (Fig. S4). Thus, Fru<sup>B</sup> appears likely to inhibit *Lgr3* median bundle expression via this fragment of an *Lgr3* intron.

Having delimited a relatively short *Lgr3* fragment that confers regulation by Fru<sup>M</sup>, we asked whether this regulation is direct. To do so, we performed EMSAs examining the binding of the Fru A, B, and C DNA-binding domains (DBDs) to probes tiled across the *R19B09.3A* fragment (Fig. 3 C–E and Fig. S5). We observed several regions that are bound by Fru-DBD-A (Fig. S5A) or Fru-DBD-B domains (Fig. 3C), suggesting Fru DBDs can directly bind sequences from the *Lgr3* gene in vitro.

We subdivided each bound probe roughly into thirds and used additional EMSAs to further refine the regions important for Fru binding. In addition, we designed competitor oligos with mutations tiled across the smaller probes (Fig. 3D and Fig. S5B). Competitors with mutations at residues unimportant for binding outcompete labeled probes, reducing or eliminating the labeled probe/protein complex. Competitors with mutations at residues important for binding leave the complex unaffected, allowing identification of necessary bases (e.g., competitor m4 in Fig. 3D). We made single base mutations in the competitor to provide

maximal resolution of binding specificity (Fig. 3E). Potential Fru binding sites have been explored previously (15, 16). The sites we identified generally agree with the consensus sites previously reported. Notably, although Dalton et al. (15) identified Fru binding motifs in *Lgr3*, it did not rise above their thresholds for responding to Fru expression, perhaps because of the small number of neurons affected.

Anticipating that binding at multiple sites may be necessary for Fru function, we mutated our identified sites individually and in multiple combinations in the *R19B09.3A* reporter (Fig. S5 E and F). Examining these combinations in females and males identified several sites necessary for expression in both sexes, but no tested single mutation or combination thereof increases expression in males to female-like levels (Fig. S5 G and H). As the fourth Fru<sup>B</sup> binding site has particularly strong effects on expression, we explored further single base changes across it, but observed minimal effects on expression (Fig. S5 G and H). We hypothesize that a transcriptional activator may bind the same sites as Fru, such that mutations of the shared binding site reduce or eliminate expression in both sexes. Alternatively, the full-length Fru<sup>M</sup> protein in vivo could require a longer binding site or additional cofactors for binding.

**Dsx<sup>F</sup> Activates and Inhibits *Lgr3* Expression in Different Abdominal Ganglion Neurons.** Although the sexually dimorphic pattern of *Lgr3* expression in the median bundle is relatively straightfor-

ward, with females having broader expression than males, we observed a more complex *Lgr3-GAL4* pattern in the abdominal ganglion, where both females and males express *Lgr3-GAL4*, but in different patterns (Fig. 4A). Mutants in *fru<sup>M</sup>* did not appear to change these *Lgr3-GAL4* abdominal ganglion expression patterns (Fig. S6A), but mutations in *dsx* did alter these patterns (Fig. 4A). As with *Lgr3* expression in the brain median bundle, we examined the expression of *Lgr3* enhancer fragment lines (Fig. 2A) to determine if any confer sex-specific expression in the abdominal ganglion. Of the five lines examined, *R17G11-GAL4* and *R17H01-GAL4* replicate subsets of the *Lgr3* pattern in the abdominal ganglion. As before, we examined how these two enhancer fragments relate to *Lgr3*, *fru*, and *dsx* to determine the basis of their sexually dimorphic expression and how it relates to the sexual dimorphisms seen in *Lgr3*.

The first of the two fragments mentioned above, *R17G11-GAL4*, is expressed in several abdominal ganglion cells in males, but not in females (Fig. 4B). *R17G11-GAL4* also directs non-dimorphic expression in the brain. To compare the abdominal ganglion expression driven by the *R17G11* enhancer fragment to that driven by *Lgr3-GAL4* and *dsx<sup>GAL4(Δ2)</sup>*, we replaced the GAL4 sequence in *R17G11-GAL4* with LexA to make *R17G11-LexA*. *R17G11-LexA* showed coexpression with *Lgr3-GAL4* in the male abdominal ganglion, but not in the female (Fig. 4C). We examined the intersection between *R17G11-LexA* and *dsx<sup>GAL4(Δ2)</sup>* as well as between *R17G11-GAL4* and *fru-LexA*, and

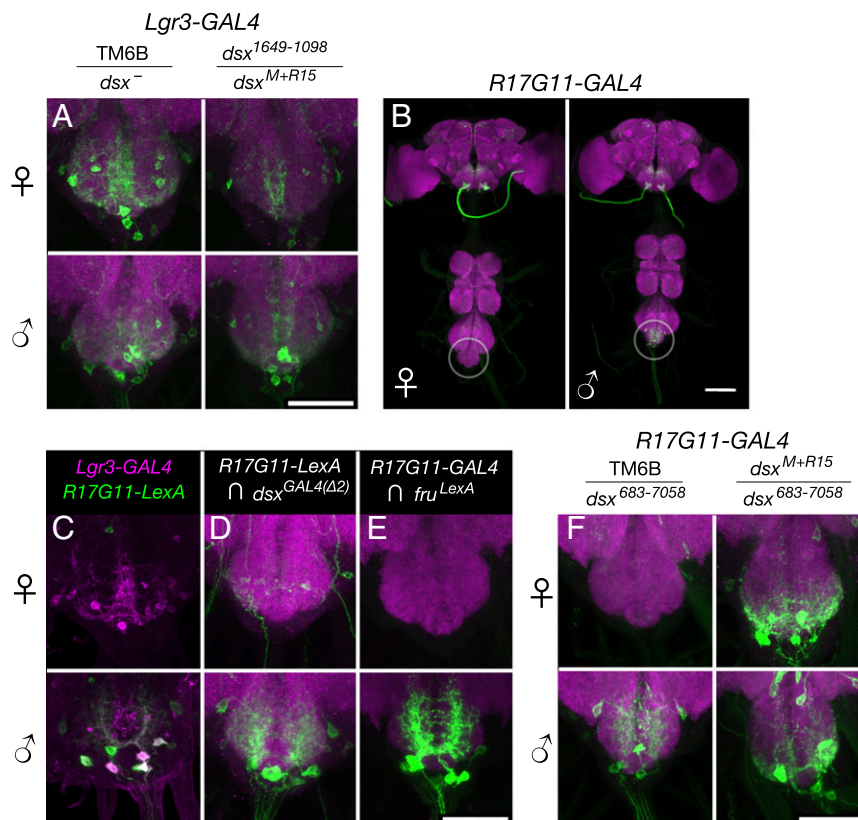


**Fig. 4.** *Lgr3-GAL4* and *R17G11-GAL4* abdominal ganglion expression depend on Dsx<sup>F</sup>. (A) *Lgr3-GAL4* (*attP40*), *UAS-myrGFP* (*su(Hw)attP5*) expression in the female and male abdominal ganglion. Left column is heterozygous for the TM6B balancer and either *dsx<sup>M+R15</sup>* or *dsx<sup>1649-1098</sup>*. Right column is heterozygous for *dsx<sup>M+R15</sup>* and *dsx<sup>1649-1098</sup>*. (Scale bar, 50  $\mu$ m.) (B) *R17G11-GAL4* (*attP2*), *UAS-myrGFP* (*attP40*) expression in females and males. Sexually dimorphic abdominal ganglion expression is circled. The brain and VNC were imaged in separate 20 $\times$  tiles and composited. (Scale bar, 100  $\mu$ m.) (C) Expression of *R17G11-LexA::p65* (*attP40*) and *Lgr3-GAL4* (*VK33*) driving *UAS-IVS-mCD8::RFP* (*attP18*) and *LexAop2-mCD8::GFP* (*su(Hw)attP8*) in females and males. Coexpression is seen in males but not females. (D) Intersection of *R17G11-LexA::p65* (*attP40*) with *dsx<sup>GAL4(Δ2)</sup>* using *LexAop2-FlpL* (*attP40*) and *UAS > stop > myrGFP* (*su(Hw)attP1*). (E) Intersection of *R17G11-GAL4* (*attP2*) with *fru<sup>LexA</sup>* using *LexAop2-FlpL* (*attP40*) and *UAS > stop > myrGFP* (*su(Hw)attP1*). (Scale bar, 50  $\mu$ m.) (F) *R17G11-GAL4* (*attP2*), *UAS-myrGFP* (*attP40*) expression in the female and male abdominal ganglion with *dsx<sup>683-7058</sup>* and either the TM6B balancer or *dsx<sup>M+R15</sup>*. (Scale bar, 50  $\mu$ m.)

in both cases we observed expression in the male abdominal ganglion, but little or none in females (Fig. 4 D and E). Examination of *R17G11-GAL4* expression in *fru<sup>M</sup>* and *dsx* loss-of-function mutants indicated that Dsx (Fig. 4F), but not Fru<sup>M</sup> (Fig. S6B), regulates *R17G11*. Unlike Fru, Dsx has functional forms in both sexes. As loss-of-function mutations of *dsx* led to expression of *R17G11-GAL4* in females, it appears that the female form of Dsx, Dsx<sup>F</sup>, either inhibits *R17G11* expression or the survival of these neurons in females.

The second of the two fragments mentioned above, *R17H01-GAL4*, showed a pattern of regulation in the abdominal ganglion opposite to that of *R17G11-GAL4*. *R17H01-GAL4* has expression in several abdominal ganglion cells in females, but fewer cells in males (Fig. 5A). As with *R17G11-GAL4*, we replaced the GAL4 in *R17H01-GAL4* with LexA to make *R17H01-LexA* to compare it with *Lgr3-GAL4* and *dsx<sup>GAL4(Δ2)</sup>*. Coexpression of *R17H01-LexA* with *Lgr3-GAL4* was seen in females, but not in

males (Fig. 5B). Comparisons of the expression patterns of *R17H01-LexA* with *dsx<sup>GAL4(Δ2)</sup>* and *R17H01-GAL4* with *fru-LexA* indicated minimal coexpression with *fru<sup>M</sup>*, but coexpression with *dsx* especially in females (Fig. 5 C and D). Examination of *R17H01-GAL4* expression in *fru<sup>M</sup>* and *dsx* loss-of-function mutants indicated that Dsx (Fig. 5E), but not Fru<sup>M</sup> (Fig. S6C), regulates *R17H01-GAL4*. Loss-of-function mutations of *dsx* largely eliminate *R17H01-GAL4* expression in the female abdominal ganglion but have no clear effect in males. Thus, it appears that Dsx<sup>F</sup> again plays the controlling role, but in this case it activates *R17H01* expression in females, as opposed to the inhibition of *R17G11*. The effects of Dsx<sup>F</sup> on *Lgr3-GAL4* expression in the abdominal ganglion may be the simple additive sum of its effects on *R17H01* and *R17G11*, with each enhancer driving expression in the appropriate subsets of neurons.

The above results indicate that Dsx regulates *Lgr3* expression in the abdominal ganglion, but do not reveal whether this regulation is

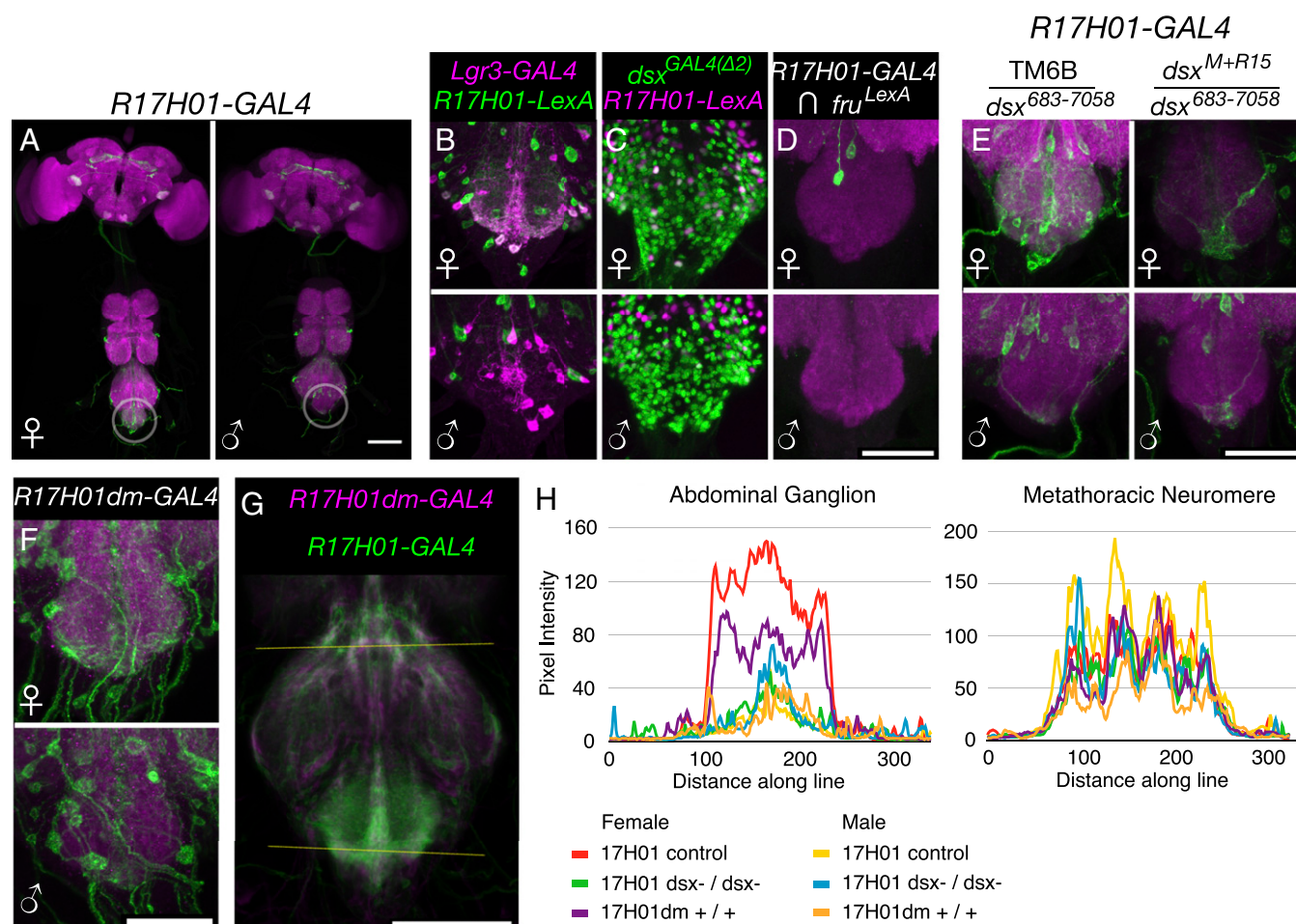


**Fig. 5.** *R17H01-GAL4* expression depends on Dsx<sup>F</sup>. (A) *R17H01-GAL4* (*attP2*), *UAS-myrGFP* (*attP40*) expression in females and males. Sexually dimorphic abdominal ganglion expression is circled. The brain and VNC were imaged in separate 20× tiles and composited. (Scale bar, 100 μm.) (B) Expression of *R17H01-LexA::p65* (*attP2*) and *Lgr3-GAL4* (*VK33*) driving *UAS-IVS-mCD8::RFP* (*attP18*) and *LexAop2-mCD8::GFP* (*su(Hw)attP8*) in females and males. Coexpression is seen in females but not males. (C) *R17H01-LexA::p65* (*attP2*), *LexAop2-IVS-nlstdTomato* (*VK22*) has some colocalization with *dsx<sup>GAL4(Δ2)</sup>*, *UAS-Stinger-GFP* in females, but less so in males. (D) Intersection of *R17H01-GAL4* (*attP2*) with *fru<sup>LexA</sup>* using *LexAop2-FlpL* (*attP40*) and *UAS > stop > myrGFP* (*su(Hw)attP1*). (Scale bar, 50 μm.) (E) *R17H01-GAL4* (*attP2*), *UAS-myrGFP* (*attP40*) expression in the female and male abdominal ganglion with *dsx<sup>683-7058</sup>* and either the TM6B balancer or *dsx<sup>M+R15</sup>*. (Scale bar, 50 μm.) (F) *R17H01dm-GAL4* (*attP2*), *UAS-myrGFP* (*attP40*) expression in the female and male abdominal ganglion. (Scale bar, 50 μm.) (G) Line scans of *R17H01-GAL4* and *R17H01dm-GAL4* expression in the metathoracic neuromere (upper line) and abdominal ganglion (lower line). *R17H01-GAL4* is shown in green, and *R17H01dm-GAL4* is in magenta. For each group (see H, below), five to seven VNCs were registered based on nc82, averaged together, and partially z-projected in preparation for line scans. (Scale bar, 100 μm.) (H) Line scan profiles of *R17H01-GAL4* and *R17H01dm-GAL4* expression in the abdominal ganglion and metathoracic neuromere. *R17H01dm-GAL4*, *UAS-myrGFP* (*attP2*) females and males were compared with a mixture of *R17H01-GAL4*, *UAS-myrGFP* (*attP40*) heterozygous controls (*dsx<sup>1649-1098</sup>/+*, *dsx<sup>683-7058</sup>/+*, and *fru<sup>LexA</sup>/+*) and *R17H01-GAL4*, *UAS-myrGFP* (*attP40*) *dsx* mutants (*dsx<sup>683-7058</sup>/dsx<sup>M+R15</sup>*, *dsx<sup>1649-1098</sup>/dsx<sup>M+R15</sup>*, and *dsx<sup>1649-1098</sup>/dsx<sup>1</sup>*).

direct, or a result of indirect effects such as Dsx-dependent cell death. We attempted to address this question, as described below. Previous work identified regions of likely Dsx DNA-binding activity and a consensus 13-bp Dsx binding motif (GCAACAATGTTGC) (5, 13, 32). The *Lgr3* locus contains three potential Dsx binding sites: a 9/13-bp partial binding site match in *R17G11* (GagACAATGTgaC, with mismatches in lowercase), and two 10- and 11-bp partial matching sites in *R17H01* (GCAACatTGaaGt and GttACAtGTTGC). We focused on *R17H01* because of its closer matches to the 13-bp motif identified previously (5). We mutated these putative binding sites to disrupt Dsx binding, and hence suggest whether Dsx directly regulates *R17H01* expression. Mutation of the *R17H01-GAL4* Dsx binding sites (changed to GCAGtgccaggGT and GTTACgcaccGC, respectively, with mutated bases in lowercase) created *R17H01dm-GAL4*, where “dm” denotes the presence of mutated DSX binding sites.

*R17H01dm-GAL4* driving *UAS-GFP* yielded a moderate decrease in female abdominal ganglion expression compared with *R17H01-GAL4* and no change in males (Fig. 5 F–H). Because the change in expression in Fig. 5F is subtle, several ventral nerve cords (VNCs) were registered together, and expression of *R17H01dm-GAL4* in the abdominal ganglion was compared with *R17H01-GAL4* in wild-type and *dsx* loss-of-function mutants (Fig. 5G). To quantitate the changes in expression, a line scan analysis was performed along the two lines shown in Fig. 5G, the upper control line and the lower line across the abdominal ganglion (Fig. 5H). *R17H01dm-GAL4* shows a reduction in expression intensity across the female abdominal ganglion, but not across the mesothoracic neuromere. This reduction was intermediate between control and *dsx* loss-of-function mutant *R17H01-GAL4* females.

Thus, it appears that Dsx<sup>F</sup> may directly regulate a fraction of *R17H01-GAL4*, and hence *Lgr3*, expression. However, other aspects of *Lgr3* abdominal ganglion expression may be regulated indirectly or by enhancers in *R17H01* outside the Dsx binding sites. The latter case was recently observed with Dsx regulation of *Fmo-2* expression, in which both a Dsx binding site and nearby enhancers were necessary for the full pattern of sexually dimorphic expression (12).

**Female *Lgr3*-Expressing Neurons Regulate Sexual Behavior.** To begin to understand the functional significance of sex-specific *Lgr3* regulation, we stimulated *Lgr3* neurons using the thermogenetic activator *UAS-dTrpA1* and assayed changes in courtship behavior. We placed virgin male and female pairs in courtship chambers and (i) measured latency to courtship initiation by males (indicated by their first wing extension directed at females), (ii) measured latency to successful copulation, and (iii) looked for other obvious changes in behavior. Activation in females of *R17H01-GAL4* neurons inhibits female receptivity to male courtship, as indicated by delayed or no copulation during the observation period (Fig. 6). Control females consisted of *pBDPGAL4u* (which lacks an enhancer insertion) with *UAS-dTrpA1* and *R17H01-GAL4* without *UAS-dTrpA1*. Performance of the two controls was not significantly different ( $P = 0.2$  for courtship latency and  $P = 0.4$  for copulation latency, by log-rank test,  $n = 130$  and 47, respectively), and the genotypes were pooled for further comparisons. Although males initiated courtship of *R17H01 > dTrpA1* and control females at indistinguishable speeds ( $P = 0.15$ , log-rank test) (Fig. 6A), *R17H01 > dTrpA1* female receptivity to courtship was significantly reduced at the Trp-activating temperature of 29 °C ( $P < 0.001$ , log-rank

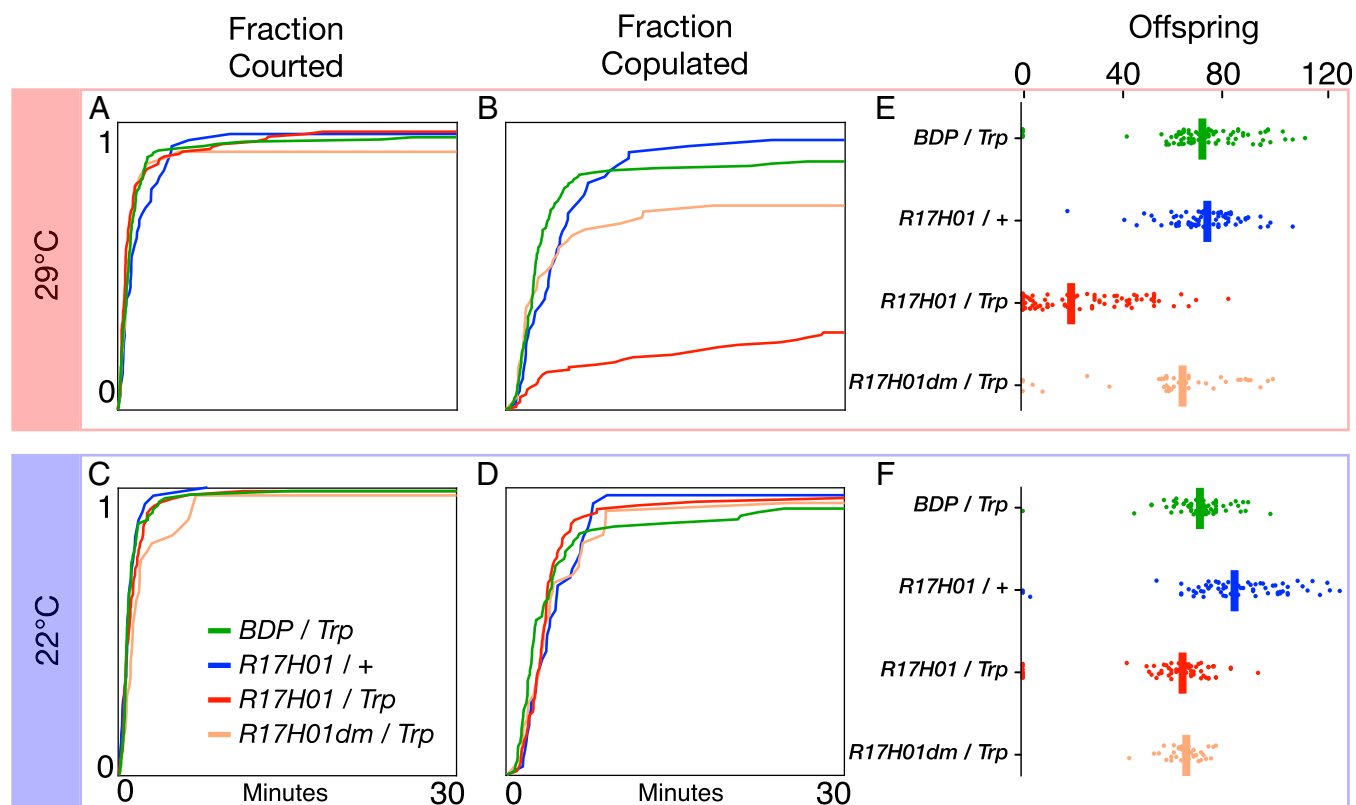


**Fig. 6.** Activation of *R17H01-GAL4* neurons reduces female receptivity and fecundity. Canton-5 males were individually placed with females in courtship chambers. Latency to initiation of male courtship, measured by first wing extension, and successful copulation were measured at (A and B) 29 °C and (C and D) 22 °C. Pairs were transferred to a fly vial with food and maintained at (E) 29 °C or (F) 22 °C until offspring were counted at the pharate pupal stage. *R17H01-GAL4*, *UAS-dTrpA1* females had significantly delayed copulation and reduced fecundity at 29 °C. Survival plots in (A–D) show cumulative percentage completion over 30 min. Fecundity plots in (E and F) show each female’s number of offspring, along with a bar indicating the average for each group.

test,  $n = 116\text{--}177$ ) (Fig. 6B). No difference was seen between the experimental and control groups in courtship or copulation latency at 22 °C, where Trp is inactive (courtship latency  $P = 0.3$ , copulation latency  $P = 0.6$ , log-rank test,  $n = 78\text{--}115$ ) (Fig. 6C and D).

After observing their courtship, as described above, we briefly anesthetized the male/female pairs and placed them into food vials to measure their fecundity. Pairs were maintained at 29 °C or 22 °C until offspring were counted at the pharate adult stage. *R17H01 > dTrpA1* females displayed significantly lower fecundity than *pBDP GAL4 > dTrpA1* or *R17H01/+* females at 29 °C ( $P < 0.001$  for both, Kruskal–Wallace test then Dunn post hoc with Bonferroni correction,  $n = 82\text{--}90$ ) (Fig. 6E). This difference was not simply because of a failure to copulate: rather than being a mix of completely infertile and unaffected females, most *R17H01 > dTrpA1* females produced fewer offspring, (Fig. 6E). At 22 °C, fecundity was somewhat variable between control genotypes, but all were significantly above *R17H01 > dTrpA1* at 29 °C ( $P < 0.001$  for each, Kruskal–Wallace test then Dunn post hoc with Bonferroni correction) (Fig. 6F).

Although the effects of Dsx-binding-site mutations on *R17H01dm-GAL4* expression were subtle, we asked whether they were sufficient to alter the phenotype observed in tests of *R17H01 > dTrpA1* females (Fig. 6). At 29 °C, *R17H01dm > dTrpA1* females were courted as promptly as *R17H01 > dTrpA1* females ( $P = 0.2$ , log-rank test,  $n = 48\text{--}116$ ) (Fig. 6A) but showed a strong increase in receptivity ( $P < 0.001$ , log-rank test) (Fig. 6B). *R17H01dm > dTrpA1* female receptivity was statistically indistinguishable from controls ( $P = 0.3$ , log-rank test,  $n = 48\text{--}178$ ) (Fig. 6B). At 22 °C there was a slight, but significant, delay in courtship toward *R17H01dm > dTrpA1* females ( $P = 0.043$ , log-rank test,  $n = 36\text{--}78$ ) (Fig. 6C), but no difference in receptivity ( $P = 0.3$ , log-rank test) (Fig. 6D). Similarly, *R17H01dm > dTrpA1* females showed a significant recovery in fecundity at 29 °C compared with *R17H01 > dTrpA1* ( $P < 0.001$ , Kruskal–Wallace test then Dunn post hoc with Bonferroni correction,  $n = 47\text{--}90$ ) (Fig. 6E), but no difference at 22 °C ( $P = 1$ , Kruskal–Wallace test then Dunn post hoc with Bonferroni correction,  $n = 36\text{--}69$ ) (Fig. 6E and F). Thus, although GFP expression was only partially reduced in *R17H01dm* flies, it appears that the Dsx binding site-dependent effects on *R17H01* expression account for most or all of its effects on female receptivity and fecundity.

Other recent studies have also examined the abdominal ganglion neurons necessary for female reproductive behavior in *Drosophila* (18, 19, 33–35). One question is whether the neurons we report here are the same or different from those previously reported. Gou et al. (33) focused on ascending neurons from the reproductive tract, and both Feng et al. (34) and Bussell et al. (35) reported stimulation of neurons favoring receptivity. In contrast, we observed that stimulation of *R17H01-GAL4* neurons inhibits receptivity, suggesting the neurons examined here differ from the ones reported above.

Rezával et al. also identified two populations of Dsx-expressing neurons in the female abdominal ganglion that when activated cause females to become less receptive (18, 19). The relationship between the two populations, labeled by either the *ET<sup>FLP250</sup>* enhancer trap flippase or octopaminergic/tyramineric *Tdc2-GAL4* driver, is not entirely clear, but their overall morphology does not strongly resemble that of *Lgr3-GAL4* or *R17H01-GAL4*. We compared the intersection of *ET<sup>FLP250</sup>* and *dsx<sup>GAL4(Δ2)</sup>* with that of *ET<sup>FLP250</sup>* and *Lgr3-GAL4* or *R17H01-GAL4* (Fig. S7). *ET<sup>FLP250</sup>* intersected with *R17H01-GAL4* does show a pattern similar to a subset of *ET<sup>FLP250</sup>* intersected with *dsx<sup>GAL4(Δ2)</sup>*, but *ET<sup>FLP250</sup>* intersected with *Lgr3-GAL4* does not. Thus, it appears that *ET<sup>FLP250</sup>* coexpresses with separate populations of neurons in the two drivers, despite their otherwise strong correspondence (Fig. 5B). It is also notable that Rezával et al. (18) observed a strong effect of *ET<sup>FLP250</sup>, dsx<sup>GAL4</sup>, UAS > stop > TrpA1* in females inhibiting the initiation of male courtship, whereas we observed prompt courtship initiation toward

*R17H01-GAL4, UAS-dTrpA1* females. As a result, although we cannot exclude the possibility that our observed reproductive phenotypes result from effects on the same neurons, it appears unlikely.

## Discussion

We have shown that *Dsx<sup>F</sup>* and *Fru<sup>M</sup>* regulate the expression of *Lgr3* in separate populations of *Drosophila* neurons. *Fru<sup>B</sup>* inhibits *Lgr3* expression in the median bundle in males, whereas *Dsx<sup>F</sup>* inhibits *Lgr3* expression in one population of abdominal ganglion neurons and activates expression in another population. This combined regulation of *Lgr3* marks a point of convergence in sex determination after the *Dsx/Fru* split. Furthermore, we found that activation of *Lgr3*-expressing neurons inhibits female receptivity toward male courtship and lowers female fecundity, indicating the functional importance of these neurons.

In vitro binding of *Fru-DBD-B* to *R19B09.3A* suggests *Fru<sup>M</sup>* could directly regulate *Lgr3* expression in vivo in the median bundle. However, the functional consequences of this regulation remain unclear. *Fru<sup>M</sup>*-expressing median bundle neurons have previously been shown to play an important role in coordinating steps of male courtship (36). Preventing *Lgr3* expression in these neurons may play a role in specifying their male-specific function. Alternatively, *Lgr3* median bundle expression could help specify female behavior, with *Fru<sup>M</sup>* inhibition in males preventing a male-specific side effect.

Expression analysis of *Drosophila Lgr3* and *Lgr4* at the level of whole tissue was recently reported (37). Although significant differences in expression were reported between males and females, these were outside the central nervous system. The largest reported adult dimorphisms were higher male expression in salivary glands and higher female expression in the fat body. A lack of nervous system changes reported by Van Hiel et al. (37) may not conflict with our results, because only a small number of neurons were affected in our observations, and the changes in the abdominal ganglion were bidirectional.

The distant homology of *Lgr3* to mammalian relaxin receptors RXFP1 and RXFP2 presents the possibility of related function, as well as related structure. These receptors and their ligands, relaxin and insulin-like peptide 3, respectively, are necessary for normal reproductive physiology in the male testis and female ovary, along with other functions (reviewed in refs. 23 and 38). This homology has led to the proposal that insulin-like peptides, especially Dilp8, may function as ligands for *Lgr3* in *Drosophila* (39). Dilp8 has been implicated in the regulation of developmental timing and growth in the larva (40, 41), and *Lgr3* has recently been found to be necessary for this Dilp8 function (42–44). *Lgr3* mutants appear to develop similarly to *dilp8* mutants and prevent effects of Dilp8 overexpression, and some evidence has been found for direct interaction between them (44; but see ref. 43).

It is unclear whether Dilp8 signaling is also important for *Lgr3*'s reproductive function, but it is notable that Dilp8 is highly expressed by the adult female ovary (45). Thus, we hypothesize that the ovaries may signal their state via Dilp8 to *Lgr3*-expressing neurons in the abdominal ganglion, which then regulate aspects of female reproductive behavior. Regulation of *Lgr3* expression by the sex-determination hierarchy may thus pattern the neural components of a sex-specific signaling pathway.

## Materials and Methods

**Transgenic *Drosophila*.** *Lgr3-GAL4::VP16* was generated by recombination-mediated replacement of the coding portion of the first *Lgr3* coding exon with *GAL4::VP16* in a bacterial artificial chromosome, which was then inserted into the *Drosophila* genome at defined attP sites. Other *GAL4* reporter stocks were generated by standard methods (46). See *SI Materials and Methods* for detailed transgenic methods.

**Immunohistochemistry, in Situ Hybridization, and Microscopy.** For immunohistochemistry, adult fly central nervous systems were dissected in Schneider's insect medium and fixed in 4% (wt/vol) paraformaldehyde. Primary and secondary antibodies were applied to label neuropil and neuronal membranes.

For in situ hybridization, pharate pupal flies were frozen in OCT compound, cryostat sectioned, and transferred to adhesive slides. They were exposed to DIG-labeled sense and antisense probes from *Lgr3* and processed with the PerkinElmer TSA Plus Cyanine 3 System. GFP was then labeled by standard immunohistochemical methods. All samples were imaged on a Zeiss LSM 710 and processed using Fiji and Computational Morphometry Toolkit. See *SI Materials and Methods* for a detailed description.

**Protein Expression and EMSA.** Fru A, B, and C DNA-binding domains were obtained by RT-PCR from wild-type flies and expressed in bacteria. EMSA was performed as described previously (5). See *SI Materials and Methods* for further description.

**Courtship and Fecundity Assays.** Four- to 7-d-old flies were aspirated into standard courtship chambers and allowed to recover. The divider between

males and females was removed, and the latency until courtship initiation and successful copulation were measured. After filming, flies were CO<sub>2</sub>-anesthetized and moved into standard food vials. Numbers of pupal offspring were counted one week later. See *SI Materials and Methods* for a full description of behavioral methods.

**ACKNOWLEDGMENTS.** We thank Dave Mellert and Kevin McGowan for help planning in situ experiments; Xiaorong Zhang for in situ probes; Susan Michael for sectioning and in situ hybridization; Heather Dionne and Gerald Rubin for GAL4 and LexA lines and constructs; Barret Pfeiffer and Gerald Rubin for providing pJFRC106; members of the B.S.B. laboratory, David Mellert, and Troy Shirangi for feedback; and Alison Howard for administrative support. The *Drosophila* Genomics Resource Center, supported by National Institutes of Health Grant 2P40OD010949-10A1, is thanked for supplying cDNA clones. This study was supported in part by the Howard Hughes Medical Institute for funding.

- Sturtevant A (1915) Experiments on sex recognition and the problem of sexual selection in *Drosophila*. *J Anim Behav* 5(5):351–366.
- Erickson JW, Quintero JJ (2007) Indirect effects of ploidy suggest X chromosome dose, not the X:A ratio, signals sex in *Drosophila*. *PLoS Biol* 5(12):e332.
- Yamamoto D, Koganezawa M (2013) Genes and circuits of courtship behaviour in *Drosophila* males. *Nat Rev Neurosci* 14(10):681–692.
- Cline TW, Meyer BJ (1996) Vive la différence: Males vs females in flies vs worms. *Annu Rev Genet* 30:637–702.
- Luo SD, Shi GW, Baker BS (2011) Direct targets of the *D. melanogaster* D5XF protein and the evolution of sexual development. *Development* 138(13):2761–2771.
- Chatterjee SS, Uppendahl LD, Chowdhury MA, Ip P-L, Siegal ML (2011) The female-specific doublesex isoform regulates pleiotropic transcription factors to pattern genital development in *Drosophila*. *Development* 138(6):1099–1109.
- Burtis KC, Coschigano KT, Baker BS, Wensink PC (1991) The doublesex proteins of *Drosophila melanogaster* bind directly to a sex-specific yolk protein gene enhancer. *EMBO J* 10(9):2577–2582.
- Coschigano KT, Wensink PC (1993) Sex-specific transcriptional regulation by the male and female doublesex proteins of *Drosophila*. *Genes Dev* 7(1):42–54.
- Hutson SF, Bownes M (2003) The regulation of *yp3* expression in the *Drosophila melanogaster* fat body. *Dev Genes Evol* 213(1):1–8.
- Williams TM, et al. (2008) The regulation and evolution of a genetic switch controlling sexually dimorphic traits in *Drosophila*. *Cell* 134(4):610–623.
- Shirangi TR, Dufour HD, Williams TM, Carroll SB (2009) Rapid evolution of sex pheromone-producing enzyme expression in *Drosophila*. *PLoS Biol* 7(8):e1000168.
- Luo SD, Baker BS (2015) Constraints on the evolution of a *doublesex* target gene arising from doublesex's pleiotropic deployment. *Proc Natl Acad Sci USA* 112(8):E852–E861.
- Clough E, et al. (2014) Sex- and tissue-specific functions of *Drosophila doublesex* transcription factor target genes. *Dev Cell* 31(6):761–773.
- Ito H, et al. (2012) Fruitless recruits two antagonistic chromatin factors to establish single-neuron sexual dimorphism. *Cell* 149(6):1327–1338.
- Dalton JE, et al. (2013) Male-specific Fruitless isoforms have different regulatory roles conferred by distinct zinc finger DNA binding domains. *BMC Genomics* 14(1):659.
- Neville MC, et al. (2014) Male-specific fruitless isoforms target neurodevelopmental genes to specify a sexually dimorphic nervous system. *Curr Biol* 24(3):229–241.
- Vernes SC (2014) Genome wide identification of fruitless targets suggests a role in upregulating genes important for neural circuit formation. *Sci Rep* 4(4412):4412.
- Rezával C, et al. (2012) Neural circuitry underlying *Drosophila* female postmating behavioral responses. *Curr Biol* 22(13):1155–1165.
- Rezával C, Nojima T, Neville MC, Lin AC, Goodwin SF (2014) Sexually dimorphic octopaminergic neurons modulate female postmating behaviors in *Drosophila*. *Curr Biol* 24(7):725–730.
- Zhou C, Pan Y, Robinett CC, Meissner GW, Baker BS (2014) Central brain neurons expressing *doublesex* regulate female receptivity in *Drosophila*. *Neuron* 83(1):149–163.
- Dolan J, et al. (2007) The extracellular leucine-rich repeat superfamily; a comparative survey and analysis of evolutionary relationships and expression patterns. *BMC Genomics* 8(1):320.
- Luo C-W, et al. (2005) Bursicon, the insect cuticle-hardening hormone, is a heterodimeric cystine knot protein that activates G protein-coupled receptor LGR2. *Proc Natl Acad Sci USA* 102(8):2820–2825.
- Anand-Ivell R, Ivell R (2014) Regulation of the reproductive cycle and early pregnancy by relaxin family peptides. *Mol Cell Endocrinol* 382(1):472–479.
- Robinett CC, Vaughan AG, Knapp J-M, Baker BS (2010) Sex and the single cell. II. There is a time and place for sex. *PLoS Biol* 8(5):e1000365.
- Rideout EJ, Dornan AJ, Neville MC, Eadie S, Goodwin SF (2010) Control of sexual differentiation and behavior by the *doublesex* gene in *Drosophila melanogaster*. *Nat Neurosci* 13(4):458–466.
- Lee G, et al. (2000) Spatial, temporal, and sexually dimorphic expression patterns of the *fruitless* gene in the *Drosophila* central nervous system. *J Neurobiol* 43(4):404–426.
- Mellert DJ, Knapp J-M, Manoli DS, Meissner GW, Baker BS (2010) Midline crossing by gustatory receptor neuron axons is regulated by *fruitless*, *doublesex* and the Roundabout receptors. *Development* 137(2):323–332.
- Cachero S, Ostrovsky AD, Yu JY, Dickson BJ, Jefferis GSXE (2010) Sexual dimorphism in the fly brain. *Curr Biol* 20(18):1589–1601.
- Yu JY, Kanai MI, Demir E, Jefferis GSXE, Dickson BJ (2010) Cellular organization of the neural circuit that drives *Drosophila* courtship behavior. *Curr Biol* 20(18):1602–1614.
- Jefferis A, et al. (2012) A GAL4-driver line resource for *Drosophila* neurobiology. *Cell Reports* 2(4):991–1001.
- Billeter J-C, et al. (2006) Isoform-specific control of male neuronal differentiation and behavior in *Drosophila* by the *fruitless* gene. *Curr Biol* 16(11):1063–1076.
- Erdman SE, Chen HJ, Burtis KC (1996) Functional and genetic characterization of the oligomerization and DNA binding properties of the *Drosophila* doublesex proteins. *Genetics* 144(4):1639–1652.
- Gou B, Liu Y, Guntur AR, Stern U, Yang C-H (2014) Mechanosensitive neurons on the internal reproductive tract contribute to egg-laying-induced acetic acid attraction in *Drosophila*. *Cell Reports* 9(2):522–530.
- Feng K, Palfreyman MT, Häsemeyer M, Talsma A, Dickson BJ (2014) Ascending SAG neurons control sexual receptivity of *Drosophila* females. *Neuron* 83(1):135–148.
- Bussell JJ, Yapici N, Zhang SX, Dickson BJ, Vosshall LB (2014) Abdominal-B neurons control *Drosophila* virgin female receptivity. *Curr Biol* 24(14):1584–1595.
- Manoli DS, Baker BS (2004) Median bundle neurons coordinate behaviours during *Drosophila* male courtship. *Nature* 430(6999):564–569.
- Van Hiel MB, Vandersmissen HP, Proost P, Vanden Broeck J (2015) Cloning, constitutive activity and expression profiling of two receptors related to relaxin receptors in *Drosophila melanogaster*. *Peptides* 68:83–90.
- Ivell R, Kotula-Balak M, Glynn D, Heng K, Anand-Ivell R (2011) Relaxin family peptides in the male reproductive system—A critical appraisal. *Mol Hum Reprod* 17(2):71–84.
- Veenstra JA (2014) The contribution of the genomes of a termite and a locust to our understanding of insect neuropeptides and neurohormones. *Front Physiol* 5:454.
- Colombani J, Andersen DS, Léopold P (2012) Secreted peptide Dilp8 coordinates *Drosophila* tissue growth with developmental timing. *Science* 336(6081):582–585.
- Garelli A, Gontijo AM, Miguéla V, Caparros E, Dominguez M (2012) Imaginal discs secrete insulin-like peptide 8 to mediate plasticity of growth and maturation. *Science* 336(6081):579–582.
- Colombani J, et al. (2015) *Drosophila* Lgr3 couples organ growth with maturation and ensures developmental stability. *Curr Biol* 25(20):2723–2729.
- Garelli A, et al. (2015) Dilp8 requires the neuronal relaxin receptor Lgr3 to couple growth to developmental timing. *Nat Commun* 6:8732.
- Vallejo DM, Juarez-Carreño S, Bolívar J, Morante J, Dominguez M (2015) A brain circuit that synchronizes growth and maturation revealed through Dilp8 binding to Lgr3. *Science* 350(6262):aac6767.
- Chintapalli VR, Wang J, Dow JAT (2007) Using FlyAtlas to identify better *Drosophila melanogaster* models of human disease. *Nat Genet* 39(6):715–720.
- Pfeiffer BD, et al. (2008) Tools for neuroanatomy and neurogenetics in *Drosophila*. *Proc Natl Acad Sci USA* 105(28):9715–9720.
- Pfeiffer BD, et al. (2010) Refinement of tools for targeted gene expression in *Drosophila*. *Genetics* 186(2):735–755.
- Barolo S, Carver LA, Posakony JW (2000) GFP and beta-galactosidase transformation vectors for promoter/enhancer analysis in *Drosophila*. *Biotechniques* 29(4):726, 728, 730, 732.
- Meissner GW, et al. (2011) Functional dissection of the neural substrates for sexual behaviors in *Drosophila melanogaster*. *Genetics* 189(1):195–211.
- Barolo S, Castro B, Posakony JW (2004) New *Drosophila* transgenic reporters: Insulated P-element vectors expressing fast-maturing RFP. *Biotechniques* 36(3):436–440, 442.
- Pan Y, Robinett CC, Baker BS (2011) Turning males on: Activation of male courtship behavior in *Drosophila melanogaster*. *PLoS One* 6(6):e21144.
- Anand A, et al. (2001) Molecular genetic dissection of the sex-specific and vital functions of the *Drosophila melanogaster* sex determination gene *fruitless*. *Genetics* 158(4):1569–1595.
- Pan Y, Meissner GW, Baker BS (2012) Joint control of *Drosophila* male courtship behavior by motion cues and activation of male-specific P1 neurons. *Proc Natl Acad Sci USA* 109(25):10065–10070.
- Mellert DJ, Robinett CC, Baker BS (2012) *doublesex* functions early and late in gustatory sense organ development. *PLoS One* 7(12):e51489.
- Baker BS, Hoff G, Kaufman T, Wolfner MF, Hazelrigg T (1991) The *doublesex* locus of *Drosophila melanogaster* and its flanking regions: A cytogenetic analysis. *Genetics* 127(1):125–138.
- Hildreth PE (1965) *doublesex*, a recessive gene that transforms both males and females of *Drosophila* into intersexes. *Genetics* 51(4):659–678.

